The Path Density of Interhemispheric Surface-to-Surface Transport. Part I: Development of the Diagnostic and Illustration with an Analytic Model

MARK HOLZER

Columbia University, New York, New York

(Manuscript received 21 July 2008, in final form 14 January 2009)

ABSTRACT

A new path-density diagnostic for atmospheric surface-to-surface transport is formulated. The path density η gives the joint probability that air whose last surface contact occurred on patch Ω_i at time t_i will make its next surface contact with patch Ω_f after a residence time $\tau \in (\tau, \tau + d\tau)$ *and* that it can be found in d^3r during its surface-to-surface journey. The dependence on τ allows the average surface-to-surface flow rate carried by the paths to be computed. A simple algorithm for using passive tracers to determine η is developed. A key advantage of the diagnostic is that it can be computed efficiently without an adjoint model and using only a moderately large number of tracers. The nature of the path density is illustrated with a one-dimensional advection–diffusion model. In Part II of this study, the path density diagnostic is applied to quantify interhemispheric transport through the troposphere and stratosphere.

1. Introduction

An understanding of interhemispheric transport is essential for the interpretation of the observed global-scale structure of long-lived anthropogenic trace gases, which have their dominant sources in the Northern Hemisphere (NH). Many studies have interpreted the observed meridional gradients of tracers such as CO_2, chlorofluorocarbons (CFCs), and SF_6 in terms of a single interhemispheric exchange time (e.g., Heimann and Keeling 1986; Maiss and Levin 1994; Bowman and Cohen 1997). The underlying conceptual model for these exchange times, typically found to be on the order of 1 yr, is a simple two-box model with each box being a hemisphere (e.g., Bowman and Cohen 1997). Although such bulk time scales provide a convenient index of interhemispheric transport to assess variability and climate change, they are a very incomplete characterization of interhemispheric transport. Plumb and McConalogue (1988) emphasized that the mixing ratio at a given point is determined by an admixture of fluid elements, each of which will generally have taken a different path from the source. More recent analyses using transport Green functions show that the lag in mixing ratio between the hemispheres can be understood in terms of the moments of the distribution of times since last contact with the source region (e.g., Hall and Plumb 1994; Holzer and Boer 2001).

The large-scale transport circulation that determines interhemispheric transport has been characterized in a number of ways. Plumb and Mahlman (1987) used synthetic tracers in a general circulation model to extract the zonally averaged transport operator in terms of advection by an effective transport velocity and diffusion by an eddy-diffusivity tensor. They also showed that rapid vertical mixing and outflow aloft in the tropics facilitates rather than throttles interhemispheric transport. Bowman and Carrie (2002) and Bowman and Erukhimova (2004) used Lagrangian particle dispersion to characterize the zonally averaged transport circulation in terms of the climatological Green functions of the advective transport operator on a time scale of 10–20 days. For the stratosphere, the residual mean circulation has been defined to quantify the Brewer–Dobson circulation (e.g., Andrews et al. 1987). However, these circulation diagnostics cannot be used to predict the paths that air or tracers follow from the NH surface to the Southern Hemisphere (SH) surface or

Corresponding author address: Mark Holzer, Department of Applied Physics and Applied Mathematics, Columbia University, c/o NASA Goddard Institute for Space Studies, 2880 Broadway, New York, NY 10025.
E-mail: hm2220@columbia.edu

DOI: 10.1175/2009JAS2894.1

how fast paths with transit times of a few months differ from slow paths with transit times of years.

The key objective of this study is to quantify rigorously the surface-to-surface paths of air from the NH to the SH. Because of the advective–diffusive nature of atmospheric transport, no single surface-to-surface transit time (or simply "residence time") or finite set of paths can fully characterize the transport, and a continuous distribution of times and paths is considered. In Part I of this study, we reformulate the path-density transport diagnostic recently introduced in an oceanographic context by Holzer and Primeau (2006, 2008) so that it is suitable for efficient computation in the highly turbulent atmosphere. The diagnostic is the joint probability density $\eta(\mathbf{r}, \Omega_f, t_i + \tau|\Omega_i, t_i)$ per unit residence time τ and per unit volume (or per unit mass depending on the choice of coordinates) that a fluid element that had last surface contact on patch Ω_i at time t_i will make its next surface contact with Ω_f after a time $\tau \in (\tau, \tau + d\tau)$ *and* that it can be found in d^3r at position $\mathbf{r}$ during its surface-to-surface journey. Because η is thus the probability density of fluid elements that transit through d^3r at $\mathbf{r}$ on their way from Ω_i to Ω_f, and because each such fluid element can be thought of as being attached to the $\Omega_i \rightarrow \Omega_f$ path that it traces out, η is also the density of these paths per unit volume and per unit residence time. The density in residence time allows the determination of the residence-time-averaged surface-to-surface flow rate through volume element d^3r, whereas the density in space quantifies where the fluid can be found during its surface-to-surface journey.

In a sense, the path density may be considered an extension of the age spectrum (Hall and Plumb 1994). Broadly, the age spectrum partitions air in volume element d^3r at $\mathbf{r}$ according to the time elapsed since last contact with a specified region, whereas the path density further partitions this air according to when and where it will next contact the surface. Holzer and Primeau (2006, 2008) applied the path-density diagnostic to steady oceanic flow using a forward and adjoint ocean model. The reformulation presented here makes it feasible to dispense with the adjoint model and provides a very simple method of using passive tracers with suitable interior sources to construct numerically exact volume (or mass) averages of the path density.

2. The path density

The path density is defined for transport from surface patch Ω_i to surface patch Ω_f, where the (initial) origin patch Ω_i and the (final) destination patch Ω_f are two tiles of a suitable tiling of the earth's surface, or any other "control surface" of interest. The patches Ω_i and Ω_f can be infinitesimal area elements or individual grid cells of a numerical model, but they are typically chosen to be of much larger (e.g., continental-scale) size. For the formulation developed here, the reasons for choosing large finite patches are presentational convenience in the case of Ω_f and computational limitations in terms of the required number of tracers in the case of Ω_i. The path density provides the joint probability that fluid elements whose last surface contact occurred on patch Ω_i at time t_i will make their subsequent surface contact with Ω_f during the time interval $(t_f, t_f + dt_f)$ *and* that these fluid elements can be found in volume element d^3r at position $\mathbf{r}$ during their surface-to-surface transit. The path density is thus a joint probability density with respect to $\mathbf{r}$, Ω_f, and t_f conditioned on Ω_i and t_i. Note that the density with respect to t_f is also the density with respect to residence time $\tau = t_f - t_i$ because t_i is a fixed conditioning.

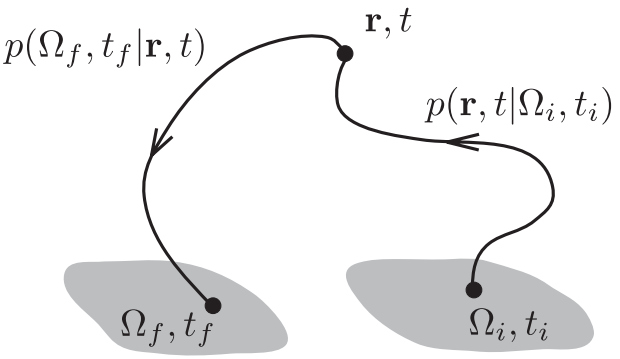

FIG. 1. The $\Omega_i \rightarrow \Omega_f$ path density at $(\mathbf{r}, t)$ is constructed from (a) the probability $p(\mathbf{r}, t|\Omega_i, t_i)d^3rdt$ of finding fluid in volume element d^3r at $\mathbf{r}$ during $(t, t + dt)$ that had last surface contact with patch Ω_i at time t_i and (b) the probability $p(\Omega_f, t_f|\mathbf{r}, t)dt_f$ that fluid that is at $\mathbf{r}$ at time t will make its next surface contact with patch Ω_f during $(t_f, t_f + dt_f)$. The path density η is obtained by multiplying $p(\Omega_f, t_f|\mathbf{r}, t)$ and $p(\mathbf{r}, t|\Omega_i, t_i)$ and marginalizing (integrating out) the time of interior transit t.

a. Probabilistic construction

This path density is constructed from two pieces of information (Fig. 1). The first piece is the probability $p(\mathbf{r}, t|\Omega_i, t_i)d^3rdt$ that fluid that had last surface contact with patch Ω_i at time t_i [referred to as "(Ω_i, t_i) air"] can be found in volume element d^3r during time interval $(t, t + dt)$. We expressed this probability in terms of its probability density function (PDF) $p(\mathbf{r}, t|\Omega_i, t_i)$ with the normalization $\int_{t_i}^{\infty} dt \int d^3r\, p(\mathbf{r}, t|\Omega_i, t_i) = 1$. (By standard convention, the PDF arguments to the right of the vertical are the conditioned variables.) The second piece of information is the probability $p(\Omega_f, t_f|\mathbf{r}, t)dt_f$ that fluid elements that are at $\mathbf{r}$ at time t make their next surface contact with patch Ω_f during $(t_f, t_f + dt_f)$.

The PDF $p(\mathbf{r}, t|\Omega_i, t_i)$ quantifies the transport from the surface to an interior volume element at $(\mathbf{r}, t)$, whereas the PDF $p(\Omega_f, t_f|\mathbf{r}, t)$ quantifies transport from $(\mathbf{r}, t)$ back to the surface. We now combine the surface-to-**r** and **r**-to-surface information to obtain the joint probability that (Ω_i, t_i) air will be found in d^3r during $(t, t + dt)$ *and* make its subsequent surface contact with Ω_f during $(t_f, t_f + dt_f)$. The corresponding PDF is given by

$$\begin{aligned} p(\mathbf{r}, t, \Omega_f, t_f|\Omega_i, t_i) &= p(\Omega_f, t_f|\mathbf{r}, t, \Omega_i, t_i)p(\mathbf{r}, t|\Omega_i, t_i) \\ &= p(\Omega_f, t_f|\mathbf{r}, t)p(\mathbf{r}, t|\Omega_i, t_i), \end{aligned} \tag{1}$$

where the first equality is the product rule for conditional probabilities and the second equality follows from the fact that $p(\Omega_f, t_f|\mathbf{r}, t, \Omega_i, t_i) = p(\Omega_f, t_f|\mathbf{r}, t)$ because the probability of making next surface contact once conditioned on $(\mathbf{r}, t)$ must be conditionally independent on where that fluid had last surface contact. In other words, once we know that the fluid is at **r** at time t, its probability of next surface contact cannot have any causal dependence on where the fluid was before it arrived at **r**.

While $p(\mathbf{r}, t, \Omega_f, t_f|\Omega_i, t_i)$ contains complete information about the surface-to-surface transport via transit volume d^3r at $(\mathbf{r}, t)$, it is very useful to reduce the dimensionality of the diagnostic for greater computational efficiency. Whereas the surface-to-surface transit time $\tau \equiv t_f - t_i$, which is also the residence time for which fluid elements are in the interior without surface contact, is of great interest, the actual time t when Ω_i fluid bound for Ω_f is in d^3r is less interesting. We therefore define the path density η by integrating out (marginalizing) the time of transit t:

$$\eta(\mathbf{r}, \Omega_f, t_f|\Omega_i, t_i) = \int_{t_i}^{t_f} dt\, p(\Omega_f, t_f|\mathbf{r}, t)p(\mathbf{r}, t|\Omega_i, t_i). \tag{2}$$

The path density is a joint PDF in the variables **r**, Ω_f, t_f with the normalization

$$\sum_{\Omega_f} \int_V d^3r \int_t^\infty dt_f\, \eta(\mathbf{r}, \Omega_f, t_f|\Omega_i, t_i) = 1, \tag{3}$$

where V is the volume of the atmosphere and Σ_{Ω_f} sums over all patches that cover the control surface of interest.

Although computationally more demanding, it is sometimes also useful to leave Ω_i as a distributed variable by replacing $p(\mathbf{r}, t|\Omega_i, t_i)$ with $p(\mathbf{r}, t, \Omega_i|t_i)$ in (2). The quantity $p(\mathbf{r}, t, \Omega_i|t_i)d^3r dt_i$ is the joint probability that a fluid element that had last contact somewhere with the surface at time t_i had this contact with Ω_i and that it is in d^3r during $(t, t + dt)$. Normalization of the path density then requires an additional sum over all Ω_i:

$$\sum_{\Omega_i} \sum_{\Omega_f} \int_V d^3r \int_t^\infty dt_f\, \eta(\mathbf{r}, \Omega_f, t_f, \Omega_i|t_i) = 1. \tag{4}$$

[In the case of infinitesimal Ω_i and Ω_f, it is convenient to define the path density also per unit first and last contact areas so that the sums of (4) can be replaced by surface integrals.] We introduce the fully surface-origin-distributed $\eta(\mathbf{r}, \Omega_f, t_f, \Omega_i|t_i)$ here primarily to make contact with the path density defined by Holzer and Primeau (2006, 2008) to which it reduces for steady flow. We will return to a comparison with the path density of Holzer and Primeau (2006, 2008) in section 4.

b. *Probabilities in terms of transport Green functions*

To compute the path density, it is very useful to express the surface-to-**r** and **r**-to-surface probability densities in terms of transport Green functions, which obey a number of useful relations (e.g., Holzer and Hall 2000). The boundary propagator Green function $\mathcal{G}(\mathbf{r}, t|\Omega_i, t_i)$ is easily computed as the passive tracer response to a pulse in surface mixing ratio that satisfies the source-free advection–diffusion equation

$$\frac{\partial}{\partial t}(\rho\mathcal{G}) + \boldsymbol{\nabla} \cdot \mathbf{J}\mathcal{G} = 0, \tag{5}$$

where ρ is the fluid density and **J** is the flux operator of the flow. For the case of advection with velocity field **u** and Fickian diffusion with diffusivity tensor **K**, the flux operator takes the form $\mathbf{J} = \rho\mathbf{u} - \rho\mathbf{K}\boldsymbol{\nabla}$. For the general flow computed by atmospheric transport models, the flux operator contains additional terms due to parameterized processes such as convection and boundary layer turbulence. The boundary propagator $\mathcal{G}$ is ''forced'' by the boundary condition

$$\mathcal{G}(\mathbf{r}_s, t|\Omega_i, t_i) = \delta(t - t_i)\Delta^2(\mathbf{r}_s, \Omega_i), \tag{6}$$

where $\mathbf{r}_s$ is surface position, $\delta(t - t_i)$ is a Dirac delta function (typically broadened to a pulse of finite width in practice), and $\Delta^2(\mathbf{r}_s, \Omega_i)$ is a two-dimensional surface mask that is unity if $\mathbf{r}_s \in \Omega_i$ and zero otherwise. Note that after the delta-function pulse ceases, $\mathcal{G}$ obeys a surface boundary condition of zero mixing ratio. Physically, $\mathcal{G}(\mathbf{r}, t|\Omega_i, t_i)dt_i$ is the mass fraction of fluid at $(\mathbf{r}, t)$ that had last surface contact with Ω_i during $(t_i, t_i + dt_i)$, and probabilistically

$$p(\Omega_i, t_i|\mathbf{r}, t) = \mathcal{G}(\mathbf{r}, t|\Omega_i, t_i). \tag{7}$$

[Note that in standard notation for Green functions the conditional variables are on the left side of the vertical bar, opposite to the convention for probabilities (e.g., Morse and Feshbach 1953)]. From $p(\Omega_i, t_i|\mathbf{r}, t)$ we can

deduce the probability of a fluid element being in d^3r during $(t, t + dt)$ conditional on having had last surface contact with Ω_i at time t_i. As shown in appendix A, Bayes' theorem can be used to interchange distributed and conditioned variables to obtain

$$p(\mathbf{r}, t|\Omega_i, t_i) = \frac{1}{\mathcal{N}} \frac{\rho(\mathbf{r}, t)}{M} \mathcal{G}(\mathbf{r}, t|\Omega_i, t_i), \tag{8}$$

where $\mathcal{N} = \mathcal{N}(\Omega_i, t_i) = M^{-1} \int_V d^3r \int_{t_i}^{\infty} dt\, \rho(\mathbf{r}, t) \mathcal{G}(\mathbf{r}, t|\Omega_i, t_i)$ is a dimensionless normalization constant, $\rho(\mathbf{r}, t)$ is the density, and M is the total mass of the atmosphere. One can also arrive at (8) from that fact the probability of finding (Ω_i, t_i) air in d^3r during dt must be proportional to the mass $d^3r\rho(\mathbf{r}, t)\mathcal{G}(\mathbf{r}, t|\Omega_i, t_i)dt_i$ of (Ω_i, t_i) air in d^3r at time t and proportional to the length of the time interval dt. By normalizing, one obtains (8); the dt_i cancels out. In appendix A, we further show that it is a simple matter to leave Ω_i a distributed variable by not conditioning on Ω_i, but for our purposes it is computationally more economical to condition on a particular last contact patch.

The mass fraction $\tilde{\mathcal{G}}(\mathbf{r}, t|\Omega_f, t_f)dt_f$ of fluid at $(\mathbf{r}, t)$ that will make its next surface contact with Ω_f during $(t_f, t_f + dt_f)$ can be computed as the tracer flux through Ω_f resulting from a unit-mass injection at $(\mathbf{r}, t)$ in the physical time-forward flow (Holzer and Hall 2000). The response to a unit-mass tracer injection at $(\mathbf{r}', t')$ is the usual point-to-point Green function $G(\mathbf{r}, t|\mathbf{r}', t')$, which obeys the passive tracer equation with a delta-function source

$$\frac{\partial}{\partial t}[\rho(\mathbf{r}, t)G(\mathbf{r}, t|\mathbf{r}', t')] + \nabla \cdot \mathbf{J}_{\mathbf{r}} G(\mathbf{r}, t|\mathbf{r}', t') = \delta(t - t')\delta^3(\mathbf{r} - \mathbf{r}'), \tag{9}$$

subject to the boundary condition $G = 0$ at the surface; the subscript on $\mathbf{J}$ indicates the variables on which it acts. Note that G has dimensions of inverse mass whereas $\mathcal{G}$ is an inverse time. A key relationship of Green functions (e.g., Holzer and Hall 2000) now expresses $\tilde{\mathcal{G}}$ as the flux of G integrated over the destination patch Ω_f:

$$\tilde{\mathcal{G}}(\mathbf{r}, t|\Omega_f, t_f) = \int_{\Omega_f} d^2r_f\, \hat{\mathbf{n}} \cdot \mathbf{J}_{\mathbf{r}_f} G(\mathbf{r}_f, t_f|\mathbf{r}, t) \equiv \mathcal{J}_f G(\mathbf{r}_f, t_f|\mathbf{r}, t), \tag{10}$$

where $\mathbf{n}$ is the surface normal. For less cumbersome notation below, we have introduced $\mathcal{J}_f \equiv \int_{\Omega_f} d^2r_f\, \hat{\mathbf{n}} \cdot \mathbf{J}_{\mathbf{r}_f}$, which is the flux operator normal to the surface integrated over patch Ω_f. In terms of the transport PDFs, we have

$$p(\Omega_f, t_f|\mathbf{r}, t) = \tilde{\mathcal{G}}(\mathbf{r}, t|\Omega_f, t_f), \tag{11}$$

so that combining (11) and (10) and substituting together with (8) into (2), we have

$$\eta(\mathbf{r}, \Omega_f, t_f|\Omega_i, t_i) = \frac{1}{\mathcal{N}M} \mathcal{J}_f \int_{t_i}^{t_f} dt\, G(\mathbf{r}_f, t_f|\mathbf{r}, t)\rho(\mathbf{r}, t)\mathcal{G}(\mathbf{r}, t|\Omega_i, t_i). \tag{12}$$

The normalization (3) of η follows from the Chapman–Kolmogorov identity (or composition property) of Green functions [appendix B; Eq. (B2)]. In the context of mixing theories, the importance of the composition property has been emphasized by Larson (1999).

c. Practical computation of the path density

The integral in expression (12) now points to a practical way for calculating η because

$$\chi(\mathbf{r}_f, t_f; \mathbf{r}; t_i) \equiv \int_{t_i}^{t_f} dt\, G(\mathbf{r}_f, t_f|\mathbf{r}, t)\rho(\mathbf{r}, t)\mathcal{G}(\mathbf{r}, t|\Omega_i, t_i) \tag{13}$$

is immediately recognizable as the tracer solution χ resulting from a source $\rho(\mathbf{r}, t)\mathcal{G}(\mathbf{r}, t|\Omega_i, t_i)\delta^3(\mathbf{r} - \mathbf{r}')$; that is,

$$\frac{\partial}{\partial t}[\rho(\mathbf{r}, t)\chi(\mathbf{r}, t; \mathbf{r}'; t_i)] + \nabla \cdot \mathbf{J}_{\mathbf{r}}\chi(\mathbf{r}, t; \mathbf{r}'; t_i) = \rho(\mathbf{r}, t)\mathcal{G}(\mathbf{r}, t|\Omega_i, t_i)\delta^3(\mathbf{r} - \mathbf{r}'), \tag{14}$$

subject to the boundary condition $\chi = 0$ at the surface. Thus, the path density at interior point $\mathbf{r}$ can be determined by computing $\mathcal{G}$ and using it as a source for tracers χ, whose flux onto Ω_f determines η through Eq. (12). We call these χ tracers "transit tracers." Tracers that are broadly similar in concept have been used to analyze moisture transport [Galewsky et al. (2005) define tracers of last saturation], and to study nonlocal mixing in the context of transilient turbulence theory (e.g., Stull 1984; Ebert et al. 1989; Stull 1993; Sobel 1999; Larson 1999).

For every point $\mathbf{r}$ for which the path density η is desired, a transit tracer χ must be computed. If η is required at every point of a typical global three-dimensional grid, this would require a prohibitively large number $N_F \sim 5 \times 10^5$ of transit tracers, and it would be more efficient to compute $\tilde{\mathcal{G}}$ as the boundary propagator for the time-reversed adjoint flow (Holzer and Hall 2000). For the adjoint calculation, a new tracer $\tilde{\mathcal{G}}$ is needed for every time t_f and every destination patch Ω_f of interest. For example, with two Ω_f patches and daily resolution in t_f over 6 yr, this would only require $N_A = 2 \times 6 \times 365 \sim 4 \times 10^3$ tracers and would thus be two orders of magnitude more efficient than the corresponding forward calculation. However, if η is only desired for a coarse, zonally averaged gridding of the atmosphere with $N_F = 180$, such as will be considered in Holzer (2009, hereafter Part II), then computing N_F transit

tracers with the forward model is an order of magnitude more efficient that the adjoint calculation, which requires the same number of surface tracers regardless of interior spatial resolution.

The computation of η is now a straightforward procedure. Consider a coarse grid that partitions the fluid domain into N_F boxes, the nth box being denoted by B_n, which defines the three-dimensional mask $\Delta_n^3(\mathbf{r})$, which is unity if $\mathbf{r} \in B_n$ and zero otherwise. (In Part II, we define such a gridding for the atmosphere in pressure coordinates using zonally symmetric boxes.) We denote the box integral of some quantity $X(\mathbf{r})$ by $\overline{X}(\mathbf{r}_n) \equiv \int_V d^3r\Delta_n^3(\mathbf{r})X(\mathbf{r})$ and the box average of X by $\hat{X} \equiv \overline{X}/v_n$, where $\mathbf{r}_n$ is the nominal position of box B_n (e.g., its geometric or mass-weighted center) and $v_n \equiv \int_V d^3r\Delta_n^3(\mathbf{r})$ is the volume of box B_n. The box-averaged path density is then given by

$$\hat{\eta}(\mathbf{r}_n, \Omega_f, t_f|\Omega_i, t_i) = \frac{1}{\mathcal{N}M}\mathcal{J}_f\hat{\chi}(\mathbf{r}_f, t_f; \mathbf{r}_n; t_i) \tag{15}$$

and the box-integrated transit tracer $\overline{\chi}$—that is, $\chi(\mathbf{r}_f, t_f; \mathbf{r}'; t_i)$ box integrated with respect to $\mathbf{r}'$—obeys

$$\frac{\partial}{\partial t}[\rho(\mathbf{r}, t)\overline{\chi}(\mathbf{r}, t; \mathbf{r}_n; t_i)] + \nabla \cdot \mathbf{J}_\mathbf{r}\overline{\chi}(\mathbf{r}, t; \mathbf{r}_n; t_i) = \rho(\mathbf{r}, t)\mathcal{G}(\mathbf{r}, t|\Omega_i, t_i)\Delta_n^3(\mathbf{r}), \tag{16}$$

from which $\hat{\chi}$ is obtained as $\hat{\chi} = \overline{\chi}/v_n$. Thus, the computation of $\hat{\eta}$ requires $N_F + 1$ tracers: $\mathcal{G}$ to label fluid that was in surface contact with Ω_i at time t_i and N_F transit tracers $\overline{\chi}$. The transit tracers obey the boundary condition of zero mixing ratio at the surface (the union of all the Ω_f) and have initial condition $\overline{\chi} = 0$. The transit tracer for each box B_n then evolves according to (16) by simply adding the source term $\mathcal{G}(\mathbf{r}, t|\Omega_i, t_i)$ to its tendency in box B_n. We emphasize that this source term is the fully spatially structured part of $\mathcal{G}$ that lies within B_n and that the transit tracers capture the formally exact box integrals. The coarse graining of the diagnostic boxes does not introduce any inaccuracies but merely limits the spatial resolution of the path-density diagnostic. (The mixing ratios of $\mathcal{G}$ and the $\overline{\chi}$ tracers are computed using the full resolution of the transport model employed.) Physically, the $\overline{\chi}$ tracers simply relabel (Ω_i, t_i) air as having been in box B_n at every time step. Any (Ω_i, t_i) air that lingers in B_n for more than a single time step is counted anew with every time step that it spends in B_n to properly account for the probability of finding (Ω_i, t_i) air in B_n (see also section b of appendix A).

d. Flow-rate density and domain-integrated densities

The fact that η can be calculated as the surface flux of the transit tracers points to a key relationship between the path density and the flow rate with which (Ω_i, t_i) air exits or enters the domain. The mass of air in d^3r at time t that had last contact with Ω_i during $(t_i, t_i + dt_i)$ is given by $dt_i d^3r\rho(\mathbf{r}, t)\mathcal{G}(\mathbf{r}, t|\Omega_i, t_i)$, whereas the mixing ratio of (Ω_i, t_i) air at point $(\mathbf{r}_f, t_f)$ resulting from this mass is given by $dt_i d^3rG(\mathbf{r}_f, t_f|\mathbf{r}, t)\rho(\mathbf{r}, t)\mathcal{G}(\mathbf{r}, t|\Omega_i, t_i)$. Applying the Ω_f-integrated flux operator $\mathcal{J}_f$ to this mixing ratio then gives the mass flow rate of the (Ω_i, t_i) air that was in d^3r at time t onto Ω_f:

$$\phi_t(\mathbf{r}, \Omega_f, t_f, \Omega_i, t_i; t)d^3rdt_i \equiv d^3rdt_i\mathcal{J}_f G(\mathbf{r}_f, t_f|\mathbf{r}, t)\rho(\mathbf{r}, t)\mathcal{G}(\mathbf{r}, t|\Omega_i, t_i). \tag{17}$$

Therefore, $dm_\phi = \phi_t d^3rdt_i dt_f$ is the mass of air that was in d^3r at time t and that was labeled on Ω_i during $(t_i, t_i + dt_i)$ and is unlabeled on Ω_f during $(t_f, t_f + dt_f)$. The rate of inflow of this air through Ω_i at time t_i is given by $dm_\phi/dt_i = \phi_{t,\uparrow}\, d^3rdt_f$, whereas the rate of outflow of this air through Ω_f at time t_f is given by $-dm_\phi/dt_f = -\phi_{t,\downarrow}\, d^3rdt_i$ (we have added subscripts $\uparrow$ and $\downarrow$ to emphasize that we consider the inflow and outflow rates, respectively). In terms of residence time $\tau = t_f - t_i$, we have $dt_f = d\tau$ for the inflow rate (specified t_i) and $dt_i = -d\tau$ for the outflow rate (specified t_f). Conservation of mass demands that the rate of inflow through Ω_i at t_i of air making the $\Omega_i \rightarrow (\mathbf{r}, t) \rightarrow \Omega_f$ trip in time $(\tau, \tau + d\tau)$ must equal the rate of outflow of that air through Ω_f at $t_f = t_i + \tau$, so that

$$\phi_{t,\uparrow}(\mathbf{r}, \Omega_f, t_i + \tau, \Omega_i, t_i; t) = \phi_{t,\downarrow}(\mathbf{r}, \Omega_f, t_f, \Omega_i, t_f - \tau; t), \tag{18}$$

as noted in its domain-integrated form by Primeau and Holzer (2006).

Because the particular time of transit t is not of interest here, we can average over all possible t to obtain the averaged flow-rate density

$$\phi(\mathbf{r}, \Omega_f, t_f, \Omega_i, t_i) \equiv \frac{1}{\tau}\int_{t_i}^{t_f} dt\mathcal{J}_f G(\mathbf{r}_f, t_f|\mathbf{r}, t)\rho(\mathbf{r}, t)\mathcal{G}(\mathbf{r}, t|\Omega_i, t_i) = \frac{1}{\tau}\mathcal{J}_f\chi(\mathbf{r}_f, t_f; \mathbf{r}, t_i), \tag{19}$$

where χ is the mixing ratio of the transit tracer associated with volume element d^3r at $\mathbf{r}$ as defined by (13) and (14). Thus, by construction, $\phi d^3rd\tau$ is the t_i-to-t_f time averaged $\Omega_i \rightarrow \Omega_f$ mass flow rate or air that passed through d^3r. Using (12) and (13), the flow-rate and path densities are related by

$$\phi = \mathcal{N}M\frac{\eta}{\tau}, \tag{20}$$

where $\mathcal{N}$ is the dimensionless normalization constant of (8) and M is the total mass of the atmosphere. The path and flux densities thus have the same spatial patterns.

Volume integrating the flow-rate density gives the simple result (see appendix B)

$$\int d^3r\phi(\mathbf{r},\Omega_f,t_f,\Omega_i,t_i)=\mathcal{J}_f\mathcal{G}(\mathbf{r}_f,t_f|\Omega_i,t_i), \tag{21}$$

which is the inflow-rate density per unit residence time of air that stays in the domain for $\tau\in(\tau,\tau+d\tau)$ until exiting (being unlabeled) at Ω_f, regardless of the interior paths taken. Integrating this further over all residence times gives the mass inflow rate from Ω_i of air destined for Ω_f regardless of residence time. However, one must be careful when Ω_i and Ω_f overlap or touch, in which case the residence-time integral of (21) diverges to infinity at zero residence time (Hall and Holzer 2003; Primeau and Holzer 2006; see also section 3).

Similarly, the volume-integrated path density

$$\int d^3r\eta(\mathbf{r},\Omega_f,t_i+\tau|\Omega_i,t_i)=\frac{\tau}{\mathcal{N}M}\mathcal{J}_f\mathcal{G}(\mathbf{r}_f,t_i+\tau|\Omega_i,t_i) \tag{22}$$

is the joint probability density of the residence time τ and next contact location Ω_f, regardless of transit location. Thus, $d\tau\int d^3r\,\eta$ is the probability that (Ω_i,t_i) air will make its next contact with Ω_f and that this occurs after residing in the atmosphere for a time $\tau\in(\tau,\tau+d\tau)$.

3. Illustration with a 1D model

It is useful to get a sense of the physical character of the path density by considering a simple idealized model. Consider one-dimensional (1D) flow at constant velocity v from point A at $x=0$ to point B at $x=L$ in the presence of constant diffusivity κ, as indicated in Fig. 2. The "control surface" consists of points A and B. This system is simple enough to admit the analytic solutions of appendix C for the Green functions and path density. The solutions depend on the Péclet number, $P=vL/\kappa$. In a zonally averaged representation of the atmosphere, the transport by large-scale eddy diffusion [e.g., Bowman (1995) shows that the transport by breaking Rossby waves is effectively diffusive] has been shown to be as important as advection by the effective transport velocity (e.g., Plumb and Mahlman 1987; Andrews et al. 1987), so a large-scale effective Péclet number on the order of unity is appropriate.

It is useful to keep in mind the particularly simple purely advective limit $P=\infty$. It is straightforward to show that for $P=\infty$ the $A\to B$ path density becomes independent of position and $\eta=\delta(\tau-L/v)/L$. This is the "conveyor limit" in which all the fluid that had last A contact resides for exactly the advective time in the domain, and the probability of finding fluid with that

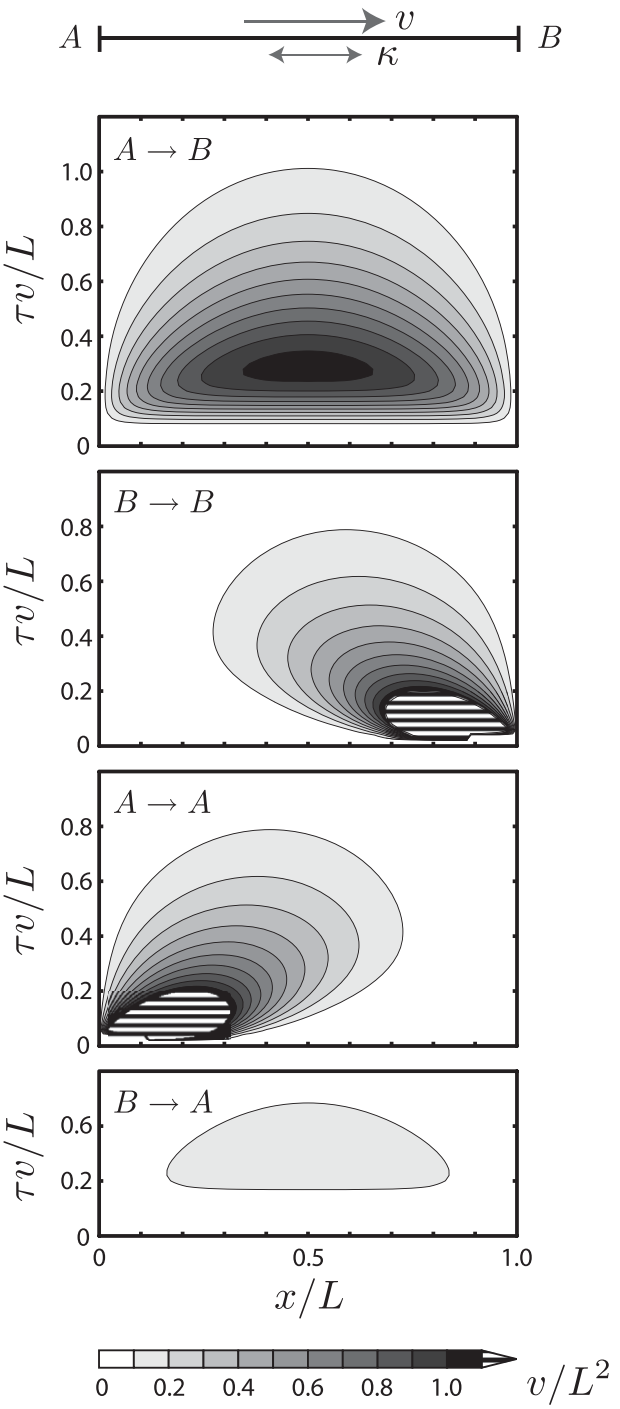

FIG. 2. The path densities of the idealized 1D model indicated in the schematic at the top. The 1D model consists of a domain of length L and a flow with velocity v and diffusivity κ, both constant. The path densities are plotted in units of v/L^2 for Péclet number $vL/\kappa=2$.

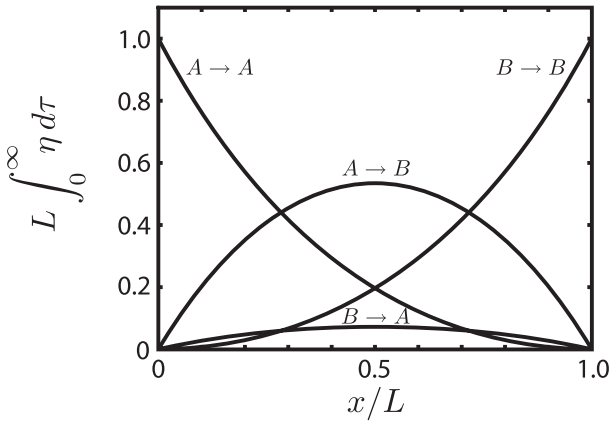

FIG. 3. Residence-time integrated, nondimensionalized path densities $L \int_0^\infty d\tau \, \eta$ for the idealized 1D model of Fig. 2 for Péclet number $P = 2$.

residence time in "volume element" dx during its $A \to B$ journey is just dx/L, independent of x. The signature of conveyor-like transport in geophysical flow is therefore a path density with minimal spatial variation along the conveyor and a narrow distribution in residence time. The more diffusive the flow, the broader the path density becomes both in residence time and in position. (The purely diffusive limit $P = 0$ requires explicit solution of the diffusion equation under appropriate boundary conditions. Some results for the $P = 0$ limit are given in appendix C.)

Some of the generic features of the path density for advective–diffusive flow are illustrated in Figs. 2 and 3 for $P = 2$. Figure 2 emphasizes that the path density is a joint density in both space and residence time. For convenience we plot the fully origin-distributed path density; the path densities conditioned on a definite last contact patch (either A or B) have the same patterns and are related via normalization constants provided in appendix C.

Consider first $\eta(x, \tau, B, A)$, the $A \to B$ path density. Note that for $P = 2$ the most probable residence time τ_m for any position x (i.e., the residence time of maximum η for fixed x) is significantly faster than the advective time (at $x = L/2$, $\tau_m L/\upsilon = 0.285$), reflecting the fact that in the presence of diffusion B is typically reached faster than by advection alone. (The ratio of the diffusive and advective times scales, $\tau_D = L^2/\kappa$ and $\tau_A = L/\upsilon$, is $\tau_D/\tau_A = P$, so τ_m/τ_A becomes proportional to P for small P.) Because of the great multiplicity of possible advective–diffusive back-and-forth paths, the path density η, as well as the underlying distributions $\mathcal{G}$ and $\tilde{\mathcal{G}}$ (not shown), are broad in τ and strongly skewed toward long τ.

Note that $\eta(x, \tau, B, A)$ is largest at $x = L/2$ and falls off to zero at A and B. To understand this basic spatial structure intuitively, it is helpful to view fluid elements as undergoing a random walk (diffusion) while drifting (advection) from A to B. $\eta(x, \tau, B, A)d\tau dx$ gives the joint probability of a fluid element labeled at A and $t_i = 0$ being found in $(x, x + dx)$ and eventually making it to B during time $t_f \in (\tau, \tau + d\tau)$. For any given τ, such A particles are not likely to be found close to A or B due to diffusion. The jittery motion of diffusion makes it likely that A particles close to either A or B will bounce into the "surface," where their (A, t_i) identity is stripped off, resulting in zones of low $A \to B$ path density close to both A and B. Particles making the A to B trip are least likely to bump into the surface in the middle of the domain, where the random back-and-forth motion of the diffusion will allow them to spend most of their $A \to B$ residence time.

It might seem surprising that $\eta(x, \tau, B, A)$ is symmetric about the midpoint, $x = L/2$, because one might expect the $A \to B$ advection to break this symmetry. Indeed, $\mathcal{G}$ and $\tilde{\mathcal{G}}$ (not plotted) are spatially skewed by advection in the expected way: For a given t the spatial maximum of the PDF of times since last A contact, $\mathcal{G}(x, t|A)$, is shifted toward B, and the more so the larger t. This is because the longer the time since last contact with A, the less likely that the particles are found close to A because they are drifting toward B. (The probability of finding A particles must, however, go to zero again close to B, because it will become increasingly likely that the random back-and-forth motion will have brought them into contact with B, where the A label is stripped off.) Similarly, the spatial maximum of the PDF of times to next contact with B, $\tilde{\mathcal{G}}(x, t|B)$, is shifted toward A, and the more so the larger t. This is because the longer the time t to next contact with B, the more likely that the particles are found ever more upstream from B, although diffusion again takes the probability to zero at A. For this 1D model, the distortion of $\mathcal{G}$ toward B has precisely the same shape as the distortion of $\tilde{\mathcal{G}}$ toward A because $\tilde{\mathcal{G}}$ evolves with the time-reversed adjoint flow, obtained here simply by $\upsilon \to -\upsilon$. The 1D model therefore has the symmetry $\tilde{\mathcal{G}}(x, t|B) = \mathcal{G}(L - x, t|A)$ and $\mathcal{G}(x, t|B) = \tilde{\mathcal{G}}(L - x, t|A)$. The convolutions of $\mathcal{G}$ and $\tilde{\mathcal{G}}$ that give the $A \to B$ and $B \to A$ path densities are thus symmetric about $x = L/2$ even in the presence of advection. The $B \to A$ path density has the same pattern as the $A \to B$ path density, but such upstream transport is exponentially less likely with increasing Péclet number.

The $A \to A$ path density $\eta(x, \tau, A, A)$ has a singularity at $x = 0$ (point A), where it reduces to $\delta(\tau)/L$. This is simply a statement of the fact that all fluid elements in contact with A must have zero transit time since last A contact, and hence zero residence time in the interior. In

the general case, it follows from the boundary conditions (6) that if Ω_i and Ω_f overlap, and $\mathbf{r}_{if}$ is a surface point on the overlap region, then $\eta(\mathbf{r}_{if}, \Omega_f, t_f|\Omega_i, t_i) = \rho(\mathbf{r}_{if}, t_i)\delta(t_f - t_i)/(\mathcal{N}M)$. For overlapping Ω_i and Ω_f and Fickian diffusion, it follows from the arguments of Hall and Holzer (2003) and Primeau and Holzer (2006) that the domain-integrated path density (22) has a $\tau^{-1/2}$ singularity as $\tau \to 0$. The corresponding $\tau^{-3/2}$ singularity of the domain-integrated flow-rate density (21) can be seen to arise from the fact that Ω_i-labeled walkers make an ever increasing number of repeat contacts with Ω_i during any finite time interval as the continuum limit is approached. The $B \to B$ path density $\eta(x, \tau, B, B)$ follows from $\eta(x, \tau, A, A)$ by symmetry.

The τ-integrated path densities for $P = 2$ are shown in Fig. 3. Note that the integrated $A \to B$ path density does not give unit probability for all x. This emphasizes that one cannot think of the path density as providing "the probability that fluid has passed through a particular volume element"—language that is misleading because the probability that A fluid passed through any dx on its way to B is unity. Instead, the path density gives the probability that A fluid can be found in dx during its $A \to B$ journey of transit time $\tau \in (\tau, \tau + d\tau)$, and the τ-integrated path density gives this probability regardless of the value of τ. The path density is higher the longer A particles spend in dx on their way to B, and, in higher dimensions, the more $\Omega_i \to \Omega_f$ particles and hence $\Omega_i \to \Omega_f$ paths pass through d^3r. The curves of Fig. 3 add to unity, or in dimensional units to $1/L$, because the probability of finding fluid in dx that had last surface contact somewhere and that will make next surface contact somewhere, regardless of when, must be dx/L and unity when integrated over x.

4. Discussion

The path density developed here differs in a number of ways from the path density defined by Holzer and Primeau (2006, 2008). The key difference is in essence the same as the difference between the widely used age spectrum of Hall and Plumb (1994) and the distribution of times since last surface contact [i.e., transit-time distribution (TTD)] (e.g., Holzer and Hall 2000; Primeau 2005). The age spectrum is constructed from the response to a single pulse during $(t_i, t_i + dt_i)$ for times $t > t_i$. The age spectrum $A(\mathbf{r}, t|t_i, \Omega_i)$ at point $\mathbf{r}$ is the normalized response $A(\mathbf{r}, t|\Omega_i, t_i) = \mathcal{G}(\mathbf{r}, t|\Omega_i, t_i)/\int_{t_i}^{\infty}\mathcal{G}dt$ as a function of the age $\tau = t - t_i$. Thus, $A(\mathbf{r}, t|\Omega_i, t_i)dt$ is the probability at $(\mathbf{r}, t)$ that the age of the fluid elements that were labeled or "born" on (Ω_i, t_i) falls in the interval $(t - t_i, t - t_i + dt)$. The age spectrum is normalized when integrated over all field times $t \in (t_i, +\infty)$. By contrast, to construct the transit-time distribution $\mathcal{G}(\mathbf{r}, t|\Omega_i, t_i)$ using a forward (as opposed to adjoint) model, one needs a new boundary tracer pulse for every interval dt_i from $t = t_i$ backward in time. The quantity $\mathcal{G}(\mathbf{r}, t|\Omega_i, t_i)dt_i$ is the mass fraction of fluid at $(\mathbf{r}, t)$ that had last Ω_i contact during $(t_i, t_i + dt_i)$ and is normalized when integrated over all source times $t_i \in (-\infty, t)$. For steady flow, the age spectrum and the transit-time distributions are identical, but for general flow the distributions can differ markedly (e.g., Holzer et al. 2003; Haine et al. 2008). The age spectrum A has a natural probabilistic interpretation, whereas the transit-time distribution is rigorously also a mass fraction. For general flow, the normalization $\int_{t_i}^{\infty}\mathcal{G}dt$ in the definition of A is not unity, which precludes the interpretation of the age spectrum as a mass fraction.

The path density defined by Holzer and Primeau (2006, 2008)—denoted here by η_0 to distinguish it from the η of this paper—bins the fluid elements in d^3r at time t according to their residence time between successive surface contacts and the places of last and next contact. The η_0 density of $\Omega_i \to \Omega_f$ paths with residence time $(\tau, \tau + d\tau)$ is constructed by multiplying the mass fraction in d^3r that had last contact with Ω_i during $(t_i, t_i + dt_i)$ with the mass fraction in d^3r that will make next contact with Ω_f during $(t_f, t_f + dt_f)$ and integrating over all times t_f and t_i that are separated by τ. Therefore, η_0 is the mass fraction in d^3r at time t that will undergo the $\Omega_i \to \Omega_f$ trip in time $(\tau, \tau + d\tau)$, regardless of the start or end time. To calculate η_0 using a forward model only would require $N_B = \tau_{\max}/\Delta t_i$ surface pulses, one for each last-contact interval Δt_i from t on back into the past for as long as the longest residence time $\tau_{\max}$ of interest, plus N_F transit tracers for each such surface pulse, a prohibitive total requirement of $N_B \times N_F$ tracers.

By contrast, here we constructed the path density η using a single surface pulse. For steady flow, η and η_0 are identical, whereas for time-dependent flow they are generally different. As discussed in section 2a, η is based on the probability $p(\mathbf{r}, t|\Omega_i, t_i)d^3rdt$ of finding in d^3r during $(t, t + dt)$ a fluid element that was labeled on Ω_i at t_i. The probability density $p(\mathbf{r}, t|\Omega_i, t_i)$ is therefore a joint spectrum of location and age $t - t_i$ that can only be interpreted as a mass fraction for steady flow. As shown in section b of appendix A, $p(\mathbf{r}, t|\Omega_i, t_i)$ can also be interpreted in terms of the "demographics" of the cohort of particles that are born on Ω_i during $(t_i, t_i + dt_i)$ and that "die" on repeat surface contact. The probability $p(\mathbf{r}, t|\Omega_i, t_i)d^3rdt$ then can be interpreted as the fraction of the cohort's available number of "mass-years" (in analogy with person-years) spent in volume element d^3r during $(t, t + dt)$. The path density η further partitions this probability according to where and when next

surface contact occurs. In terms of the (Ω_i, t_i) cohort, $\eta d^3r dt_f$ is the fraction the cohort's available mass-years spent in d^3r by those cohort particles that die on Ω_f during $(t_f, t_f + dt_f)$.

In the probability $\eta d^3r dt_f$ fluid elements are "counted" whenever they are in d^3r during their $\Omega_i \to \Omega_f$ trip. Specifically, the number of times a given fluid element is counted when it stays in d^3r for a time dt is proportional to dt. Thus, a high path density, or large average fraction of time spent in d^3r, can be achieved by having many particles pass through d^3r or by having fewer particles linger in d^3r for longer. A single particle making a quick straight-line traversal of d^3r is associated with a lower path density than a particle that slowly doodles out a more squiggly path in d^3r, as one would intuitively expect.

5. Summary and conclusions

We have developed a new path-density diagnostic of surface-to-surface transport. The path density η is defined so that $\eta(\mathbf{r}, \Omega_f, t_i + \tau|\Omega_i, t_i)d^3r d\tau$ is the joint probability that (Ω_i, t_i) air will make next surface contact with Ω_f after a surface-to-surface transit time (also referred to as residence time) $\tau \in (\tau, \tau + d\tau)$ *and* that this air can be found in d^3r during its $\Omega_i \to \Omega_f$ journey. The path density was shown to be proportional to the flow-rate density distribution ϕ, defined so that $\phi d^3r d\tau$ is the time-averaged $\Omega_i \to \Omega_f$ mass flow rate of air that passes through d^3r and that has a residence time $\tau \in (\tau, \tau + d\tau)$.

The path density can be computed with a straightforward and easily implemented algorithm using a forward transport model and a moderately large number of tracers. In essence, whenever surface-labeled air is found in one of a set of specified interior transit boxes, it is relabeled with the passive transit tracer associated with that box. The flux of the relabeled air onto the surface in the presence of a zero-mixing-ratio boundary condition then gives the residence-time partitioned probability of the air having been in the interior transit volume during its surface-to-surface journey. In this way, the exact box-averaged path density for N_F transit boxes can be computed from $N_F + 1$ passive tracers: N_F transit tracers plus a single boundary-pulse tracer that provides the interior sources of the transit tracers.

The physical character of the path density was illustrated with a simple 1D advection–diffusion model. An advectively dominated transport pathway corresponds to a path density that is spatially uniform along the pathway and narrow in residence time, whereas diffusively dominated transport produces a more diffuse path density. The jittery motion of diffusion makes it likely that fluid elements close to the surface will in fact make contact with the surface. This results in zones of low $\Omega_i \to \Omega_f$ path density close to Ω_i and Ω_f at all residence times if Ω_i and Ω_f do not overlap and in a singularity at zero residence time if Ω_i and Ω_f are identical or overlap.

Although this work is motivated by interhemispheric transport, the path-density diagnostic is general and can be applied to transport connecting any two regions of the atmosphere, or any other bounded fluid domain. In Part II of this study, we will use a transport model driven by NCEP reanalyses to compute the density of paths that connect the NH with the SH through the troposphere and stratosphere.

Acknowledgments. I thank François Primeau, Tim Hall, and Lorenzo Polvani for discussions, and three anonymous referees for comments that led to an improved manuscript. This work was supported by NSF Grants ATM-04-32514 and OCE-07-27229 and NOAA Grant NA04OAR4310118.

APPENDIX A

Conditioned Last-Contact Probability

a. Application of Bayes' theorem

Given the probability density $p(\Omega_i, t_i|\mathbf{r}, t) = \mathcal{G}(\mathbf{r}, t|\Omega_i, t_i)$ for having had last contact with (Ω_i, t_i) during $(t_i, t_i + dt_i)$ conditional on being at $\mathbf{r}$ at time t, we now construct $p(\mathbf{r}, t|\Omega_i, t_i)$, the probability density for finding a fluid particle in d^3r during $(t, t + dt)$ conditional on the particle having been at Ω_i at time t_i. Bayes' theorem states that $p(A|B)p(B) = p(B|A)p(A)$ because both sides of the equation are equal to the joint density $p(A, B)$. Applied to the probability densities of interest, we first form the joint density

$$p(\Omega_i, t_i, \mathbf{r}, t) = p(\Omega_i, t_i, |\mathbf{r}, t)p(\mathbf{r}|t)p(t), \qquad \text{(A1)}$$

where $p(\mathbf{r}|t)d^3r$ is the probability of finding a fluid element in d^3r at time t, and $p(t)dt$ is the probability that the time coordinate falls in the interval $(t, t + dt)$. The probability of finding a fluid element at time t in d^3r is proportional to the mass in d^3r so that the normalized PDF $p(\mathbf{r}|t) = \rho(\mathbf{r}, t)d^3r/M$, where M is the total mass in the fluid domain. The natural choice for the distribution of the time coordinate is uniform; that is, $p(t) = dt/T$, where T is a constant time scale longer than all times of interest (we will soon take the limit $T \to \infty$). We therefore have

$$p(\mathbf{r},t)d^3rdt = \frac{dt}{T}\frac{\rho(\mathbf{r},t)d^3r}{M}. \tag{A2}$$

The unconditional probability density $p(\Omega_i,t_i) = \int d^3r \int_{t_i}^{T} dt\, p(\Omega_i,t_i,\mathbf{r},t)$ now allows us to apply Bayes' theorem to obtain

$$p(\mathbf{r},t|\Omega_i,t_i) = \frac{p(\Omega_i,t_i,\mathbf{r},t)}{p(\Omega_i,t_i)}. \tag{A3}$$

The unspecified factor of $1/T$ cancels in both the numerator and denominator of (A3) so that we can take the limit $T \to \infty$ in the upper limit of integration to obtain Eq. (8) of the text. (In practice T merely has to exceed a few e-foldings of the exponential decay of $\mathcal{G}$.)

One can also leave Ω_i a distributed variable so that

$$p(\mathbf{r},t,\Omega_i|t_i) = \frac{p(\Omega_i,t_i,\mathbf{r},t)}{p(t_i)}, \tag{A4}$$

with $p(t_i) = \Sigma_{\Omega i}\, p(\Omega_i, \mathrm{t}_i)$. Thus, if the surface-origin distributed path density of Eq. (4) is desired, the required probability density $p(\mathbf{r}, t, \Omega_i|t_i)$ is given by Eq. (8) if $\mathcal{N}$ is replaced with $\mathcal{N}_*(t_i) \equiv \Sigma_{\Omega_i}\mathcal{N}(\Omega_i,t_i)$. The surface-origin distributed path density and the path density conditioned on air having had last surface contact with patch Ω_i are related by

$$\eta(\mathbf{r},\Omega_f,t_f,\Omega_i|t_i) = \frac{\mathcal{N}(\Omega_i,t_i)}{\mathcal{N}_*(t_i)}\eta(\mathbf{r},\Omega_f,t_f|\Omega_i,t_i). \tag{A5}$$

b. Particle demographics

The probability $p(\mathbf{r}, t|\Omega_i, t_i)d^3rdt$ may be interpreted in terms of the demographics of the cohort of fluid elements (particles for short) that are considered to have been born when they are labeled on Ω_i during $(t_i, t_i + dt_i)$ and that are considered to die when this label is removed upon repeat surface contact. The mass of the cohort at time t is given by

$$M_i(t) = dt_i \int d^3r\, \rho(\mathbf{r},t)\mathcal{G}(\mathbf{r},t|\Omega_i,t_i), \tag{A6}$$

whereas the mass of the cohort in d^3r at time t is

$$m_i(\mathbf{r},t) = dt_i d^3r \rho(\mathbf{r},t)\mathcal{G}(\mathbf{r},t|\Omega_i,t_i). \tag{A7}$$

From Eq. (8), we can now express $p(\mathbf{r}, t|\Omega_i, t_i)d^3rdt$ as

$$p(\mathbf{r},t|\Omega_i,t_i)d^3rdt = \frac{m_i(\mathbf{r},t)dt}{\mathrm{MT}}. \tag{A8}$$

The quantity $\mathrm{MT} \equiv \int_{t_i}^{\infty} M_i(t)dt$ has the interpretation as the total number of mass-years available to the cohort (in analogy with the number of person-years of a human cohort), so that the right-hand side of (A8) is the fraction of mass-years spent by the cohort in d^3r during $(t, t + dt)$.

The mass $m_{i,f}(\mathbf{r}, t)$ of the cohort in d^3r at $(\mathbf{r}, t)$ that dies on Ω_f during $(t_f, t_f + dt_f)$ is obtained by multiplying $m_i(\mathbf{r}, t)$ by $dt_f\tilde{\mathcal{G}}(\mathbf{r},t|\Omega_f,t_f)$—that is, by the fraction of fluid at $(\mathbf{r}, t)$ that makes first Ω_f contact during $(t_f, t_f + dt_f)$. Therefore, the expression

$$dt_f\tilde{\mathcal{G}}(\mathbf{r},t|\Omega_f,t_f)p(\mathbf{r},t|\Omega_i,t_i)d^3rdt = \frac{m_{i,f}(\mathbf{r},t)dt}{\mathrm{MT}} \tag{A9}$$

can be interpreted as being the fraction of the cohort's mass-years spent in d^3r during dt by those cohort particles that die on Ω_f during $(t_f, t_f + dt_f)$. Integrating (A9) over all times of transit $t \in (t_i, t_f)$ gives the probability $\int_{t_i}^{t_f} dt\tilde{\mathcal{G}}(\mathbf{r},t|\Omega_f,t_f)p(\mathbf{r},t|\Omega_i,t_i)d^3rdt_f = \eta(\mathbf{r},t,\Omega_f|\Omega_i,t_i)d^3rdt_f$, which may therefore be interpreted as the total number of mass-years spent in d^3r (regardless of when) by the cohort particles that die on Ω_f during $(t_f, t_f + dt_f)$. Equivalently, the right-hand side of (A9) may be considered to be the nondimensionalized, mass-weighted time dt spent in d^3r by cohort particles that die on Ω_f during $(t_f, t_f + dt_f)$. In this sense, the path density (obtained by integrating over all t) may be considered to be a measure of the mass-weighted time spent in d^3r during the $\Omega_i \to \Omega_f$ transport.

APPENDIX B

Volume-Integrated Flux Density

Using the fact that (e.g., Holzer and Hall 2000) $\mathcal{G}(\mathbf{r}, t|\Omega_i, t_i) = \mathcal{J}_i\mathcal{G}(\mathbf{r}, t|\mathbf{r}_i, t_i)$, we have

$$\int d^3r\, \phi(\mathbf{r},\Omega_f,t_f,\Omega_i,t_i)d^3r = \frac{1}{t_f - t_i}\int_{t_i}^{t_f} dt\mathcal{J}_f\mathcal{J}_i \int d^3r\, G(\mathbf{r}_f,t_f|\mathbf{r},t)\rho(\mathbf{r},t)G(\mathbf{r},t|\mathbf{r}_i,t_i). \tag{B1}$$

We now use the Chapman–Kolmogorov identity for G, which states that

$$\int d^3r\ G(\mathbf{r}_f,t_f|\mathbf{r},t)\rho(\mathbf{r},t)G(\mathbf{r},t|\mathbf{r}_i,t_i) = G(\mathbf{r}_f,t_f|\mathbf{r}_i,t_i), \tag{B2}$$

to obtain

$$\int d^3r\, \phi(\mathbf{r},\Omega_f,t_f,\Omega_i,t_i)d^3r = \frac{1}{t_f - t_i}\int_{t_i}^{t_f} dt\mathcal{J}_f\mathcal{J}_i G(\mathbf{r}_f,t_f|\mathbf{r}_i,t_i). \tag{B3}$$

Note that the integrand no longer depends on t, so $(\int_{t_i}^{t_f} dt)/(t_f - t_i)$ is simply unity. Re-expressing the flux of G as $\mathcal{G}$—that is, $\mathcal{J}_i\mathcal{G}(\mathbf{r}_f, t_f|\mathbf{r}_i, t_i) = \mathcal{G}(\mathbf{r}_f, t_f|\Omega_i, t_i)$—one obtains Eq. (21) of the text.

Using (19) to express ϕ in (21) in terms of the N_F box-integrated transit tracers gives

$$\sum_{n=1}^{N_F} \mathcal{J}_f \overline{\chi}(\mathbf{r}_f, t_f; \mathbf{r}_n; t_i) = (t_f - t_i)\mathcal{J}_f \mathcal{G}(\mathbf{r}_f, t_f|\Omega_i, t_i), \quad \text{(B4)}$$

which serves as a useful check on the numerical implementation of the transit tracers.

APPENDIX C

Exact Solution for 1D Advection–Diffusion

In terms of the nondimensional variables $\hat{x} \equiv x/L$, $\hat{t} \equiv \kappa t/L^2$ and the Péclet number $P \equiv vL/\kappa$, the constant-coefficient advection–diffusion equation for the nondimensional Green function $\hat{\mathcal{G}} \equiv \mathcal{G}L^2/\kappa$ of the 1D model of Fig. 2 is (suppressing the hats for clarity)

$$\left(\frac{\partial}{\partial t} + P\frac{\partial}{\partial x} - \frac{\partial^2}{\partial x^2}\right)\mathcal{G}(x, t|\Omega_i) = 0, \quad \text{(C1)}$$

with the boundary conditions

$$\mathcal{G}(\Omega_f, t|\Omega_i) = \begin{cases} \delta(t) & \text{if} \quad \Omega_f = \Omega_i, \\ 0 & \text{if} \quad \Omega_f \neq \Omega_i, \end{cases} \quad \text{(C2)}$$

where Ω_i and Ω_f are either A ($x = 0$) or B ($x = 1$). The solutions to (C1) subject to (C2) can easily be found in terms of the Laplace transform $\mathcal{L}(\mathcal{G})$. By formally expanding a factor of the generic form $(1 - e^{\sqrt{s}})^{-1}$ in $\mathcal{L}(\mathcal{G})$ as a series in $e^{\sqrt{s}}$, the inverse transform can be taken term by term and reorganized to obtain

$$\mathcal{G}(x, t|B; P) = \frac{e^{-[(x-Pt)^2+2Pt]/4t}}{\sqrt{\pi t^3}} \sum_{k_{\text{odd}}=1}^{\infty} e^{-k^2/4t}\left[k\sinh\left(\frac{kx}{2t}\right) - x\cosh\left(\frac{kx}{2t}\right)\right] \quad \text{and} \quad \text{(C3)}$$

$$\mathcal{G}(x, t|A; P) = \mathcal{G}(1 - x, t|B; -P). \quad \text{(C4)}$$

The propagators $\tilde{\mathcal{G}}$ for the time-reversed adjoint flow obey (C1) with $P \to -P$ and are given by (C3) and (C4) with $P \to -P$.

Writing Eq. (12) for the fully distributed path density in terms of $\tilde{\mathcal{G}}$, recognizing that for steady flow $\mathcal{N}_* = 1$ [cf. Eq. (A5)], and using the fact that for steady flow $\mathcal{G}$ and $\tilde{\mathcal{G}}$ depend on time only through $t - t_i$ and $t_f - t$, respectively, the surface-distributed path density for our 1D model can be written as the convolution

$$\eta(x, \tau, \Omega_f, \Omega_i) = \int_0^{\tau} dt\, \tilde{\mathcal{G}}(x, \tau - t|\Omega_f)\mathcal{G}(x, t|\Omega_i). \quad \text{(C5)}$$

This convolution can be evaluated as the inverse Laplace transform of the product of the Laplace transforms of $\mathcal{G}$ and $\tilde{\mathcal{G}}$. The inverse Laplace transform of that product was again obtained term by term after expanding its denominator as a power series. The result can be written as

$$\eta(x, \tau, B, A) = \frac{e^{P/2}e^{-\tau P^2/4}}{\sqrt{\pi\tau^3}} \sum_{k=1}^{\infty} k e^{-k^2/\tau}\left(e^{-1/4\tau}[2k\cosh(k/\tau) - \sinh(k/\tau)]\right.$$

$$\left. + e^{-(2x-1)^2/4\tau}\left\{(2x-1)\sinh\left[\frac{k(2x-1)}{\tau}\right] - 2k\cosh\left[\frac{k(2x-1)}{\tau}\right]\right\}\right), \quad \text{(C6)}$$

$$\eta(x, \tau, B, B) = \frac{2e^{-\tau P^2/4}}{\sqrt{\pi\tau^3}} \sum_{k=1}^{\infty} k e^{-k^2/\tau}\left\{e^{-x^2/\tau}\left[k\cosh\left(\frac{2kx}{\tau}\right) - x\sinh\left(\frac{2kx}{\tau}\right)\right] - k\right\}, \quad \text{(C7)}$$

$$\eta(x,\tau,A,A) = \eta(1-x,\tau,B,B), \quad \text{and} \tag{C8}$$

$$\eta(x,\tau,A,B) = e^{-P}\eta(x,\tau,B,A). \tag{C9}$$

The path densities conditional on the fluid having had last contact on either A or B are then given from (A5) by $\eta(x,\tau,\Omega_f|\Omega_i) = [1/\mathcal{N}(\Omega_i)]\eta(x,\tau,\Omega_f,\Omega_i)$, with Ω_i and Ω_f either A or B, and

$$\mathcal{N}(A) = \frac{1+e^P(P-1)}{P(e^P-1)} \quad \text{and} \tag{C10}$$

$$\mathcal{N}(B) = 1-\mathcal{N}(A). \tag{C11}$$

Note that $\mathcal{N}_* = \mathcal{N}(A) + \mathcal{N}(B) = 1$, as expected. In the purely advective limit of $P = \infty$, $\mathcal{N}(A) = 1$ and $\mathcal{N}(B) = 0$, because there is zero probability of finding fluid elements that had last contact with B in the interior of the domain and every fluid element in the interior came from A. Similarly, in the purely diffusive limit of $P = 0$, $\mathcal{N}(A) = \mathcal{N}(B) = ½$, because without advection fluid elements are equally likely to have had contact with either A or B.

The path density regardless of residence time, $\Xi(x,\Omega_f,\Omega_i) \equiv \int_0^\infty d\tau\eta(x,\tau,\Omega_f,\Omega_i)$, is given from (C5) by $\Xi(x,\Omega_f,\Omega_i) = \tilde{f}(x|\Omega_f)f(x|\Omega_i)$, where $f(x|\Omega_i) = \int_0^\infty dt\mathcal{G}(x,t|\Omega_i)$ is the mass fraction of fluid at x that had last contact with Ω_i and $\tilde{f}(x|\Omega_f) = \int_0^\infty dt\mathcal{G}(x,t|\Omega_f)$ is the mass fraction that will make first contact with Ω_f, both regardless of transit time. Solving (C1) integrated over time, or integrating and summing (C3), the fractions f are obtained as

$$f(x|B;P) = \frac{e^{xP}-1}{e^P-1}, \tag{C12}$$

$$f(x|A;P) = f(1-x,B;-P), \tag{C13}$$

with $\tilde{f}$ given by changing the sign of P. From (C13) and (C12), or by summing (C6)–(C9) integrated over τ, the residence-time integrated path densities can be obtained as

$$\Xi(x,B,A) = 2\frac{e^{3P/2}}{(1-e^P)^2}[\cosh(P/2) - \cosh(xP - P/2)], \tag{C14}$$

$$\Xi(x,B,B) = \frac{\cosh(xP)-1}{\cosh(P)-1}, \tag{C15}$$

$$\Xi(x,A,A) = \Xi(1-x,A,A), \quad \text{and} \tag{C16}$$

$$\Xi(x,A,B) = e^{-P}\Xi(x,B,A). \tag{C17}$$

Note that in the purely diffusive, self-adjoint limit ($P = 0$), the mass fractions f and $\tilde{f}$ must be consistent with a spatially constant flux of A particles toward B (where they are relabeled as B particles), and vice versa, so that $f(x|A) = \tilde{f}(x|A) = 1 - x$ and $f(x|B) = \tilde{f}(x|B) = x$. Correspondingly, the $P = 0$ limits of (C14)–(C17) are $\Xi(x,B,A) = \Xi(x,A,B) = x(1-x)$, $\Xi(x,B,B) = x^2$, and $\Xi(x,A,A) = (1-x)^2$.

REFERENCES

Andrews, D. G., J. R. Holton, and C. B. Leovy, 1987: *Middle Atmosphere Dynamics*. Academic Press, 489 pp.

Bowman, K. P., 1995: Diffusive transport by breaking waves. *J. Atmos. Sci.,* **52,** 2416–2427.

——, and P. J. Cohen, 1997: Interhemispheric exchange by seasonal modulation of the Hadley circulation. *J. Atmos. Sci.,* **54,** 2045–2059.

——, and G. D. Carrie, 2002: The mean-meridional transport circulation of the troposphere in an idealized GCM. *J. Atmos. Sci.,* **59,** 1502–1514.

——, and T. Erukhimova, 2004: Comparison of global-scale Lagrangian transport properties of the NCEP reanalysis and CCM3. *J. Climate,* **17,** 1135–1146.

Ebert, E., U. Schumann, and R. Stull, 1989: Nonlocal turbulent mixing in the convective boundary layer evaluated from large-eddy simulation. *J. Atmos. Sci.,* **46,** 2178–2207.

Galewsky, J., A. Sobel, and I. Held, 2005: Diagnosis of subtropical humidity dynamics using tracers of last saturation. *J. Atmos. Sci.,* **62,** 3353–3367.

Haine, T. W. N., H. Zhang, D. Waugh, and M. Holzer, 2008: On transit-time distributions in unsteady circulation models. *Ocean Modell.,* **21,** 35–45, doi:10.1016/j.ocemod.2007.11.004.

Hall, T. M., and R. A. Plumb, 1994: Age as a diagnostic of stratospheric transport. *J. Geophys. Res.,* **99,** 1059–1070.

——, and M. Holzer, 2003: Advective–diffusive mass flux and implications for stratosphere–troposphere exchange. *Geophys. Res. Lett.,* **30,** 1222, doi:10.1029/2002GL016419.

Heimann, M., and C. D. Keeling, 1986: Meridional eddy diffusion model of the transport of atmospheric carbon dioxide 1. Seasonal carbon cycle over the tropical Pacific Ocean. *J. Geophys. Res.,* **91,** 7765–7781.

Holzer, M., 2009: The path density of interhemispheric surface-to-surface transport. Part II: Transport through the troposphere and stratosphere diagnosed from NCEP data. *J. Atmos. Sci.,* **66,** 2172–2189.

——, and T. M. Hall, 2000: Transit-time and tracer-age distributions in geophysical flows. *J. Atmos. Sci.,* **57,** 3539–3558.

——, and G. J. Boer, 2001: Simulated changes in atmospheric transport climate. *J. Climate,* **14,** 4398–4420.

——, and F. W. Primeau, 2006: The diffusive ocean conveyor. *Geophys. Res. Lett.,* **33,** L14618, doi:10.1029/2006GL026232.

——, and ——, 2008: The path-density distribution of oceanic surface-to-surface transport. *J. Geophys. Res.,* **113,** C01018, doi:10.1029/2006JC003976.

——, I. G. McKendry, and D. A. Jaffe, 2003: Springtime transpacific atmospheric transport from East Asia: A transit-time probability density function approach. *J. Geophys. Res.,* **108,** 4708, doi:10.1029/2003JD003558.

Larson, V., 1999: The relationship between the transilient matrix and the Green's function for the advection–diffusion equation. *J. Atmos. Sci.,* **56,** 2447–2453.

Maiss, M., and I. Levin, 1994: Global increase of SF_6 observed in the atmosphere. *Geophys. Res. Lett.,* **21,** 569–572.

Morse, P. M., and H. Feshbach, 1953: *Methods of Theoretical Physics*. McGraw-Hill, 997 pp.

Plumb, R. A., and J. D. Mahlman, 1987: The zonally averaged transport characteristics of the GFDL general circulation model. *J. Atmos. Sci.,* **44,** 298–327.

——, and D. D. McConalogue, 1988: On the meridional structure of long-lived tropospheric constituents. *J. Geophys. Res.,* **93,** 15 897–15 913.

Primeau, F. W., 2005: Characterizing transport between the surface mixed layer and the ocean interior with a forward and adjoint global ocean transport model. *J. Phys. Oceanogr.,* **35,** 545–564.

——, and M. Holzer, 2006: The ocean's memory of the atmosphere: Residence-time and ventilation-rate distributions of water masses. *J. Phys. Oceanogr.,* **36,** 1439–1456.

Sobel, A., 1999: Diffusion versus nonlocal models of stratospheric mixing, in theory and practice. *J. Atmos. Sci.,* **56,** 2571–2584.

Stull, R., 1984: Transilient turbulence theory. Part I: The concept of eddy-mixing across finite distances. *J. Atmos. Sci.,* **41,** 3351–3367.

——, 1993: Review of non-local mixing in turbulent atmospheres: Transilient turbulence theory. *Bound.-Layer Meteor.,* **62,** 21–96.